Journal of Rubber Research (2023) 26:55–70
https://doi.org/10.1007/s42464-023-00192-9

ORIGINAL PAPER

# Performance evaluation of micro/nano-silica filled silicone rubbers aged under multiple environmental stresses and bipolar DC voltage

**Atif Mahmood**[1] · **Shahid Alam**[1]

Received: 12 July 2022 / Accepted: 13 February 2023 / Published online: 25 February 2023


## Abstract

For the outdoor insulation of high voltage transmission lines, insulating materials made of high-temperature vulcanized silicone rubber (HTV-SiR) are used all over the world. To enhance the performance of these base polymers, fillers of various sizes, concentrations and dimensions are added. In this study, four different types of HTV-SiR materials, one unfilled and three reinforced with silica of micro/nano size were used. Followed by preparation of the samples, aging was performed by placing them in a specially designed weathering chamber with various stresses and bipolar DC voltage for 5000 h. To diagnose integrity of the aged materials, different types of measurements based on hydrophobicity classification, leakage current, mechanical analysis, thermal tests, Fourier transform infrared (FTIR) spectroscopy and scanning electron microscopy (SEM) were conducted. Results of the hydrophobicity classification revealed $S_3$ to be most hydrophobic having HC2 class under the influence of bipolar DC voltage, whereas, sample $S_1$ was the most hydrophilic resulting in HC4 and HC5 under negative and positive DC voltages, respectively. Similarly, the lowest leakage currents of 5.56 µA and 5.81 µA were recorded for sample $S_3$ after being aged under negative DC and positive DC voltages, respectively. The %age decrease in tensile strength recorded for samples $S_1$, $S_2$, $S_3$ and $S_4$ was 32.3, 25.32, 23.56 and 27.12, respectively, under the positive DC voltage. Thermogravimetric analysis exhibited the least decrease of %yield from 49.3% to 48.9% and 48.4% for sample $S_3$ under negative and positive DC voltages, respectively. Additionally, according to FTIR spectroscopic investigation, hybrid composite $S_3$ kept the highest intactness in siloxane backbone (Si–O–Si) linkages, with a drop in its peak of 37% for positive DC and 11.2% for negative DC. In contrast to the co-filled composites $S_2$ and $S_3$ with improved surface morphology, samples $S_1$ and $S_4$ indicated voids, cracks, increased roughness and structural damages.

**Keywords** Silicone rubber · Silica · Co-filled composites · Environmental stresses · Hydrophobicity and anti-aging

## Introduction

For transporting bulk of electric power, high voltage direct current (HVDC) based transmission lines are used nowadays all around the globe. This is because of the advantages that are associated with this technology like fewer number of conductors, absence of skin effect, interconnection with alternating current (AC) grid, high efficiency, etc. Furthermore, remotely located renewable energy sources (wind, solar, hydro) can be linked to the main grid more efficiently and economically using this technology. HVDC transmission systems are matured over the years because of the tremendous improvements in power electronics converters [1, 2]. Several HVDC transmission lines are installed worldwide and are increasing with the passage of time [3]. Among these, one project is being installed between Lahore to Matiari by the National Transmission and Dispatch Company (NTDC) in Pakistan.

To implement HVDC technology for the transportation of electrical energy, a more reliable and long-lasting insulation system is required. The reason being higher degradation of insulators due to accumulation of more pollutants on their surfaces [4]. Different research studies have shown that the effect of DC voltage on the long-term performance of insulators is stronger than the AC voltage [5, 6]. The emergence of polymeric insulators for high voltage outdoor insulation has increased due to their lighter weight, high temperature withstands capability, good mechanical strength and dielectric properties as well as having high hydrophobicity [7, 8].

✉ Atif Mahmood
atifmahmood@cuisahiwal.edu.pk

[1] Ghulam Ishaq Khan Institute of Engineering Sciences and Technology, Topi 23460, Pakistan

Among these, silicone rubber (SiR) materials are gaining popularity because their superior hydrophobicity resists the flow of leakage current and occurrence of the surface flashovers [9–11]. Moreover, SiR coatings are also used to enhance the hydrophobicity of ceramic insulators, facilitating thus the suppression of leakage current as well as improve the pollution performance [12–15].

Gubanski et al. studied different types of polymers like epoxy resin, RTV-SiR, HTV-SiR and EPDM under the influence of UV radiation. They also analyzed the surface partial discharge behavior of each sample and revealed that RTV- and HTV-SiR samples are more stable than the other polymers [16]. In another work, authors aged HTV-SiR under UV radiation and concluded that this polymer is suitable for many years for outdoor insulation [17]. Despite of all the advantages of SiR insulators, they are prone to degradation in the environment having multiple stresses. For their performance enhancement, different types of reinforcing fillers were incorporated in multiple research studies. As a result of the conducted analyses, it was observed that several factors including type, size, shape, orientation and concentration of fillers improve the properties/characteristics of base polymers [18, 19]. The inclusion of micro-sized fillers enhances the dielectric, mechanical, and thermal properties of insulators.

With the enlargement of micro-sized fillers, the inter-particle spacing increases which ultimately improves certain properties [20]. Moreover, the addition of a smaller concentration of nano-fillers is more effective than the larger concentration of micro-fillers [21]. To enhance the desired properties of polymeric insulators, various types of micro- and nano-sized fillers have been employed by different researchers [22–25]. The main objective is to select a filler that can improve more effectively the dielectric, thermal, mechanical and hydrophobic properties of base polymers. Silica is the most prominent filler for the enhancement of erosion performance, anti-tracking capability, thermal stability and mechanical properties [26–29]. It is shown that HTV-SiR containing nano-silica has better weather-resistant ability as compared to its micro-silica filled counterpart. Moreover, for the performance improvement of HTV-SiR, a mixture of both micro- and nano-sized fillers have also been investigated [30]. The conducted analysis revealed stronger resistant against aging of the hybrid composites than the materials filled with only one filler in the harsh environments such as that of Karachi, Pakistan.

Under AC applied voltage, the effect of multiple environmental stresses on the long-term aging behavior of various polymeric insulators has been studied by different researchers [31–39]. However, for DC stress, such data are insufficient for the implementation of polymeric composites in HVDC transmission lines. Although, some efforts of lab accelerated aging for 5000 h have been reported in [40–42]. Nevertheless, the data of long-term aging, particularly related to HTV-SiR filled with different compositions of nano/micro-silica is rather inadequate.

Having identified the research gap, this study is conducted to perform lab accelerated aging on HTV-SiR composites for a period of 5000 h in the simulated environment of Multan, Pakistan. The aging behavior was analyzed simultaneously under the application of both positive and negative DC voltages (bipolar DC) to investigate the polarity effect. For the experimentation, four types of silicone rubber samples having different proportions of micro-and nano-silica were prepared. The test samples were mounted in a specially designed weather chamber, where they were exposed to UV radiation, salt-fog, temperature, humidity and acid rain. Thereafter, the integrity of the samples was analyzed with the help of different characterization techniques. These included hydrophobicity classification, leakage current, mechanical and thermal analyses, water immersion tests and FTIR spectroscopy. Results of the conducted diagnosis are presented and discussed. Furthermore, a comparative assessment of the different studied scenarios is made.

## The experiment

### Preparation of test samples

The base material high-temperature vulcanized silicone rubber (HTV-SiR) was procured from the Dow Corning (USA) while, the micro/nano-silica fillers were bought from Sigma Aldrich (USA). The sizes of the nano-silica and micro-silica used were 12 nm and 5 µm, respectively. For the preparation of HTV-SiR composites, two methods used were compounding and mixing of materials. Firstly, the micro/nano-silica fillers were placed in a 100 ml solution of ethanol and then, they were stirred for 20 min mechanically. HTV-SiR was mixed with the fillers and ultrasonication was performed for 30 min to make a homogenous mixture. For the removal of ethanol, the mixture was heated at a temperature of 100 °C for one hour. Thereafter, a shear blender was used for the purpose of blending. The speed of blending was increased gradually to 150 rpm for the extraction of the lumps from the mixture and the blending time was kept as 20 min. Followed by this step, a hardener was mixed with the prepared solution. The mixture was then poured into hot steel molds to shape the samples that were $50 \times 40 \times 3$ mm$^3$ in size and 50 g in weight. The steel molds were placed at room temperature for 24 h to set the composites. For the experimentation, one unfilled HTV-SiR sample and three HTV-SiR composites were prepared. Specifications of the test samples are provided in Table 1.

**Table 1** Specifications of the studied materials

| Material | Base polymer | Micro-silica | Nano-silica |
|---|---|---|---|
| $S_1$ | HTV-SiR | – | – |
| $S_2$ | HTV-SiR | 5 wt.% | 6 wt.% |
| $S_3$ | HTV-SiR | 15 wt.% | 6 wt.% |
| $S_4$ | HTV-SiR | – | 6 wt.% |

## Environmental chamber

An environmental chamber made up of acrylic sheet, schematically shown in Fig. 1, having dimensions of 2 × 1x1.5 $m^3$ was developed for the aging analysis of fabricated composites. The multiple stresses applied on the test samples included DC voltage, UV radiation, temperature, salt-fog, humidity and acid rain. The former was obtained by rectifying secondary voltage of a center-tapped step-up transformer having a rating of 220 V/ 5 kV. The DC voltage with both positive and negative polarities was applied to the copper strips, holding the test sample. UV radiations were applied with the help of four UVA-340 fluorescent lamps. A Lutron light meter was used to check the required intensity of UV radiations in the chamber. For adjusting temperature in the chamber, four electrical heating rods of 500-watts were installed along with the sensor and controller. The latter was used to maintain the required temperature level. Moreover, a humidifier together with a sensor and controller was used to maintain the required humidity level. For salt-fog and acid rain, a nozzle was placed at an appropriate position in the chamber to spray all the samples after equal time intervals during the aging period. The acid rain was applied using an HCL solution having a pH value of 4.5. As per IEC 61,109, the samples were energized with a creepage distance of 30 mm/kV [43]. Two cycles, one for the winter and the other for summer were designed using the data taken from the Pakistan's meteorological department to apply various stresses in the chamber. Details of the environmental factors constituting the weather cycles are given in Table 2.

## Diagnostic techniques

### Hydrophobicity classification

To evaluate the performance of insulators, hydrophobicity analysis is very essential. Accumulative effects of the multiple stresses may influence surface characteristics of the samples, causing them to become hydrophilic. Therefore, hydrophobicity was analyzed after each cycle of the aging

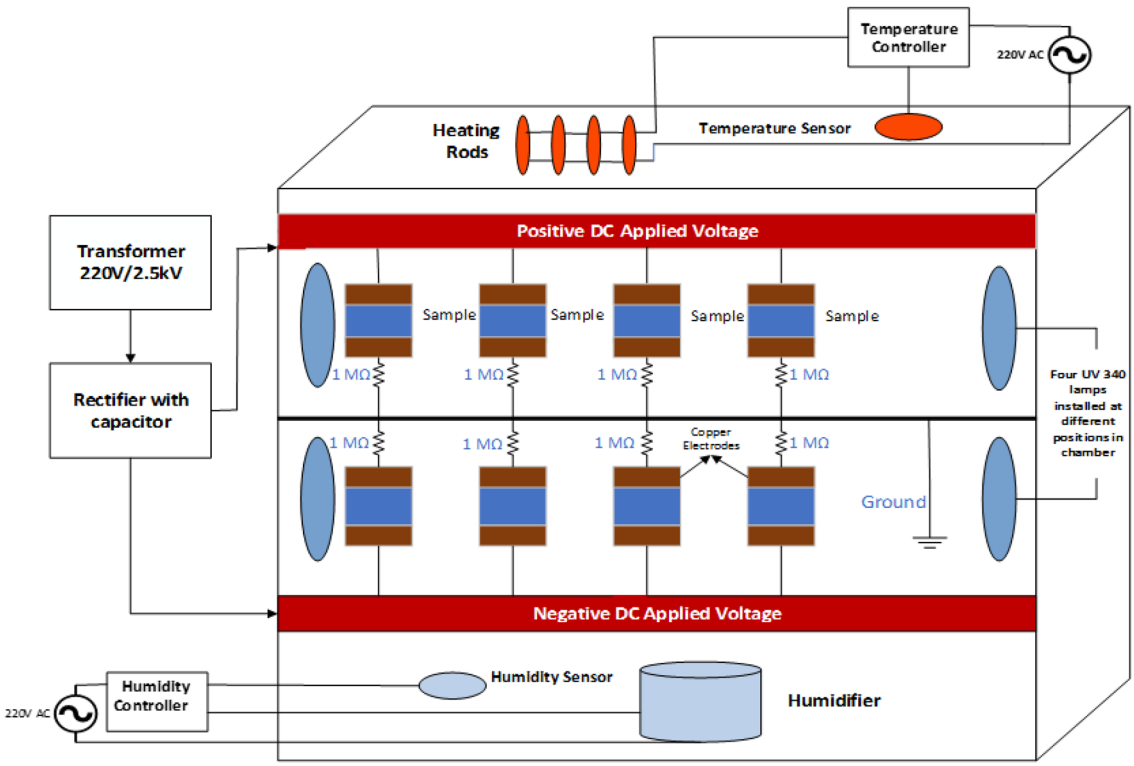


**Fig. 1** Schematic illustration of the environmental chamber having arrangements for applying both polarities of DC voltage and various types of environmental stresses

**Table 2** Summer and winter cycles of Multan designed using the data of Meteorological department of Pakistan

| Parameter/factor | Winter cycle | Summer cycle |
|---|---|---|
| Temperature (°C) | 37.24 | 49.62 |
| Relative humidity (%) | 51 | 53 |
| UV-radiation (5 mW/cm$^2$) | 8 h | 12 h |
| Acid rain (4.5 pH) | 2 | 4 |
| Salinity of fog (6000 µS/cm) | 3 | 1 |

Note that digits in the last two columns represent the number of times acid rain and salt-fog were applied during each cycle

period with the help of the Swedish Transmission Research Institute (STRI) hydrophobicity classification guide [44].

According to the standard test procedure, samples were sprayed with the tap water for 20 s, followed by capturing of their high-quality images within 10 s. Thereafter, the images were compared with the standard images given in the STRI hydrophobicity guide. According to the guide, there are seven classes of hydrophobicity ranging from HC1 to HC7. HC1 being the most hydrophobic and HC7, the most hydrophilic [44].

## Leakage current

To quantify the effect of multiple stresses on the performance of studied materials, leakage current analysis was performed. In the experimental arrangement, as high voltage was applied to energize each sample, therefore, an indirect method to measure leakage current we adopted. In the procedure followed, a resistor of 1 MΩ was connected in series with each sample and voltage drop was measured across it. A multimeter model UT-70B was used for this purpose and data were recorded after every cycle throughout the aging period.

## Mechanical properties

To analyze the effect of applied stresses on mechanical properties of the test samples, tensile strength and elongation at break (EAB) were measured. Data were recorded both before and after exposing the materials to aging. For the measurements, Instron-4465 test machine was used. Moreover, samples were cut in a dumbbell-shaped structure following IS-3400 standard [45].

## Thermal analysis

Thermal stability of the test samples both prior to and post multiple stress aging was analyzed using SDT-Q600 simultaneous TGA/DSC analyzer. Using this diagnostic technique, variation in the weight of samples with the rise in temperature was recorded. The range of temperature was kept from 25 to 900 °C with a constant increase of 10 °C per minute. Temperature-based derivative of the data was also taken to conduct differential thermogravimetric analysis (DTG) of the samples. Moreover, to avoid measurement errors, experiments were performed in a closed chamber filled with nitrogen, where its flow rate was kept as 50 ml min$^{-1}$.

## Water immersion tests

To check water repellency of the studied materials, two tests were performed both before and after the aging. These were 2-h boiling water test at 100 °C and 24-h water immersion test at 25 °C, conducted following ASTM-D570 [46, 47]. It is worth highlighting here that prior to each type of test, sample was cleaned with distilled water and then dried in a desiccator for a week time. Thereafter, water immersion tests were performed and weight of the sample was measured. From the obtained result, %age change in weight was calculated using the expression given as

$$M(t) = \left[\frac{w_t - w_o}{w_o}\right] \times 100$$

where M(t) represent %age absorption of water and $w_t$ and $w_o$ are masses of the sample after and before the test, respectively.

## FTIR spectroscopy

FTIR spectroscopy was conducted to analyze changes in the molecular structure of the test samples due to multiple stress aging effects. For this purpose, FTIR spectrometer IRTracer-100 (Shimadzu) was used. Data showing absorption peaks vs. wavenumbers were recorded both before and after aging of the samples.

## SEM analysis

SEM is a diagnostic technique used for studying surface topography to spot morphology of the materials. In the test procedure, high-energy electron beam scans the sample in a raster scanning pattern to produce SEM micrographs. Electron beam interacts with the surface atoms of the sample to produce signals, containing information of its topography and composition. In the present study, high grade SEM micrographs were captured using the FEI Quanta FEG-250 ESEM machine. Moreover, prior to the collection of data, gold was sputtered on the sample's surface.

## Results and discussion

### Hydrophobicity classification

Collected data of hydrophobicity classification of all the test samples are shown in Fig. 2. The vertical axis represents the class of hydrophobicity, HC1 being the most hydrophobic and HC7, the most hydrophilic. Similarly, the horizontal axis shows the accelerated multi-stressed lab aging duration, where 672 h is equivalent to one field year. In the figure, values are shown at the multiple of 762 h as well as at 0 h (represent unaged sample) and after complete aging period (5000 h). As seen, in general, hydrophobicity for all the studied materials decreases with the increasing duration of aging. Moreover, the loss is dependent on the composition of the samples as well as on the polarity of the applied voltage. A slight recovery phenomenon can also be noticed after the aging period of 3360 h.

Analyzing the data for individual samples, it can be seen that for sample $S_1$ (unfilled material), loss of hydrophobicity is the highest. On the other hand, among the additionally filled samples, $S_3$ (doped with 15 wt.% micro-silica and 6 wt.% nano-silica) shows the lowest decrease in its hydrophobicity. While, the resistance against loss of hydrophobicity is relatively small for materials $S_2$ and $S_4$. Furthermore, it can be observed that degradation of the test samples under positive DC voltage is stronger as compared to the negative DC. For example, for sample $S_1$ after 5000 h of aging, hydrophobicity class under positive DC is HC5, while under

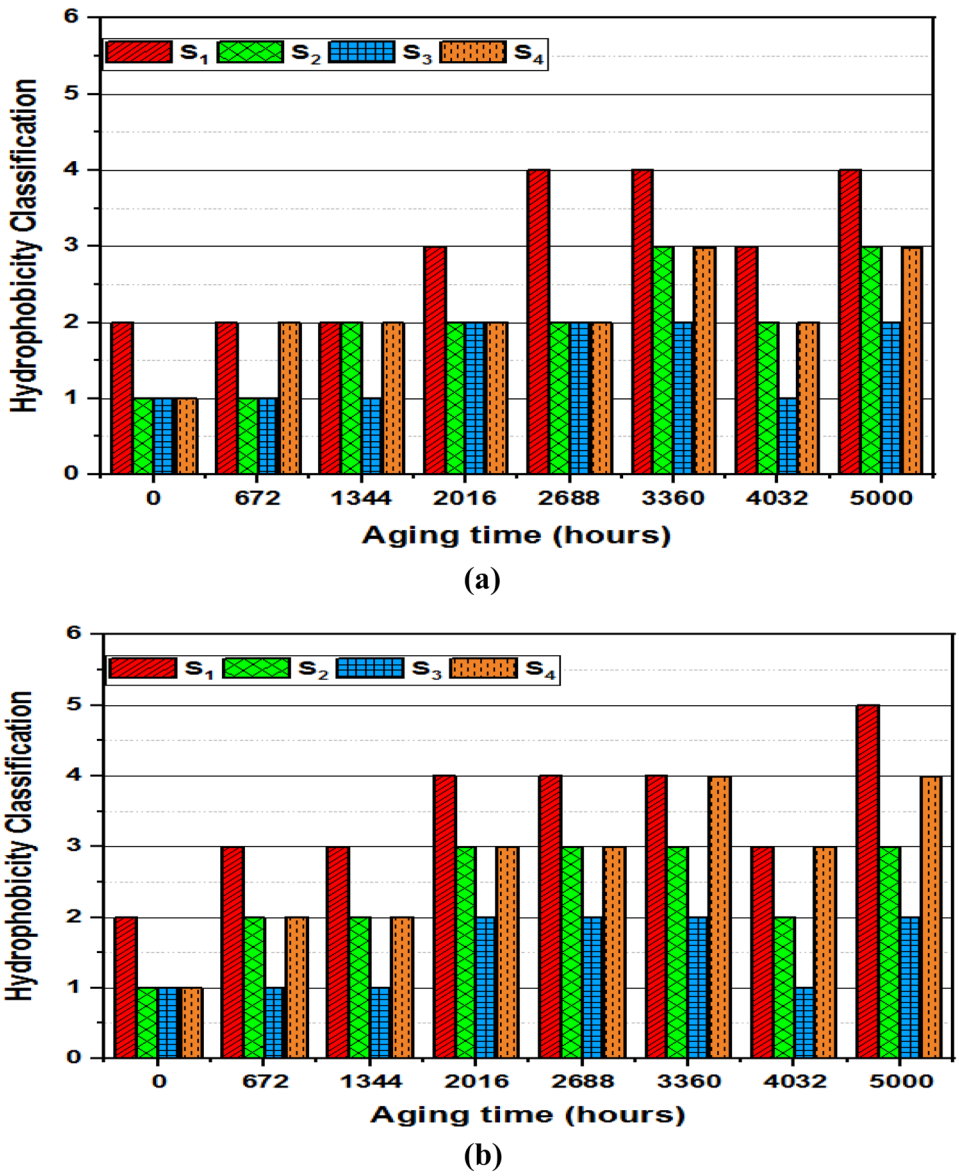


**Fig. 2** Hydrophobicity classification of the studied materials aged under (**a**) negative DC and (**b**) positive DC voltages

negative DC, it is HC4. Similar observations can also be noticed for the other samples as well.

Reasons for the loss of hydrophobicity can mainly be associated with the applied UV radiation and thermal stress in the environmental chamber, causing degradation of low molecular weights (LMWs) of the samples and also initiate oxidation processes on their surfaces. Moreover, the recovery phenomenon is due to the movement of LMWs from the bulk of materials toward their surfaces [48]. As far as polarity effect (stronger deterioration of the test samples under positive DC voltage than the negative DC) is concerned, it can be linked with the depolymerization and reduction of methyl group in the molecular structure of HTV-SiR [49].

## Leakage current

Measured values of the leakage current for the studied materials are shown in Fig. 3. Inferring the data, it can be seen that all the values exist within the range of micro-amperes. Moreover, current increases with the increasing aging period, being dependent on the sample's composition and polarity of the applied voltage. The only exception is after 3360 aging hours, where a slight decrease can be observed. Quantitatively, the highest change (in the total aging period) occurs for sample $S_1$ (unfilled sample) and the lowest, for sample $S_3$ (doped with 6 wt.% nano-silica and 15 wt.% micro-silica). Polarity effect is also noticeable. For example, after the aging period of 5000 h, leakage current for sample $S_1$ under positive DC voltage is 8.12 µA. While, it is close to 7.5 µA under negative DC. Overall, the lowest current of 5.56 µA was obtained for sample $S_3$ under negative DC voltage.

The above-described results show that hybrid composites $S_2$ and $S_3$, reinforced with micro- and nano-sized silica filler, suppresses leakage current more effectively than the other studied samples. The reason being the relatively better interaction of filler particles with the base matrix. Moreover, variation of the leakage current is in accordance with the hydrophobicity classification of the test samples. The increasing trend is due to the degradation of low molecular weights and synergetic impact of multiple stresses. This may also be associated with breaking of C–H and Si–$CH_3$ bonds in the molecular structure of HTV-SiR [9].

Polarity effect, showing stronger deterioration of test samples under positive DC stress than the negative DC, is in line with that reported in [6]. The reason being the quicker rate of charge/ion (occurs in air due to numerous background ionization processes as well as other reasons) deposition and accumulation of pollutants on the surface of the insulator [50]. Other possibility might be the electrolytic process (caused by the application of salt-fog and acid rain) in multi-stress aging, affecting surface condition more adversely under positive DC stress as compared to the negative DC as is also reported in [51].

## Mechanical properties

The measured values of tensile strength and elongation at break (EAB) for the aged and unaged materials are presented in Figs. 4a and 5a, respectively. As seen, by reinforcing base matrix with the filler particles, its mechanical properties enhance. The relatively highest values (of both tensile strength and EAB) are obtained for hybrid composite $S_3$ (filled with 6 wt.% nano-silica and 15 wt.% micro-silica) and the lowest, for unfilled sample $S_1$. For the other two materials S2 and S4, the values are in between. Moreover, by exposing the test samples to multiple stresses, their mechanical properties deteriorate. The decline in tensile strength and EAB could be associated with the chain scissions, cause sample's surface to lose its rubbery structure, and oxidation processes stimulated by the UV radiations and other stresses in the environmental chamber [52]. To quantify the decrease in tensile strength and EAB, %age values calculated with respect to the data obtained for unaged samples are presented in Figs. 4b and 5b, respectively. As seen, reduction is the minimum for hybrid composite $S_3$ and the maximum for sample $S_1$ (without any filler), regardless of the polarity of DC voltage. This can be attributed to the stronger interaction of hydrogen bonds of silica filler having silanol groups with the polymer matrix having OH groups [53]. Thus, movement of the main polymer chain is restricted, giving rise to the tensile strength of the studied samples.

Likewise other measurements (described above), effect imposed by the positive DC stress is stronger than the negative DC. For example, after performing aging for 5000 h, the decrease in tensile strength for sample $S_1$ under positive DC and negative DC voltages is 19.78% and 32.3%, respectively. While, the corresponding percentage decreases in EAB are 21.9% and 30.9. This trend is similar even for the other studied samples of HTV-SiR as well.

## Thermal analysis

Thermographs of the studied materials before and after their exposure to environmental stresses, obtained using the procedure outlined in Sect. "Thermal Analysis", are shown in Fig. 6. Data of both the TGA and DTG are presented with different scales on the y-axis. Inferring TGA curves, it can be seen that weight of the test samples decreases with the rise in temperature. The maximum loss occurs in the temperature range of 410 ˚C to 550 ˚C. While, both below and above this range, the change is rather weak. The weight loss can mainly be associated with the breakage of methyl ($CH_3$) group from the molecular structure of base polydimethylsiloxane (PDMS) [54].

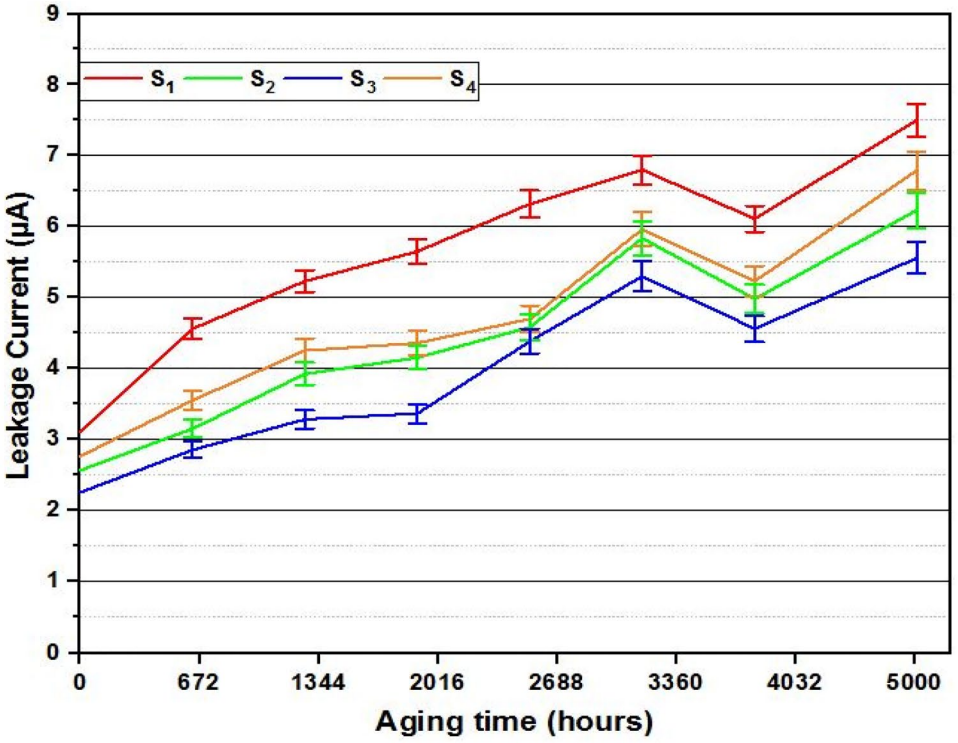


(a)

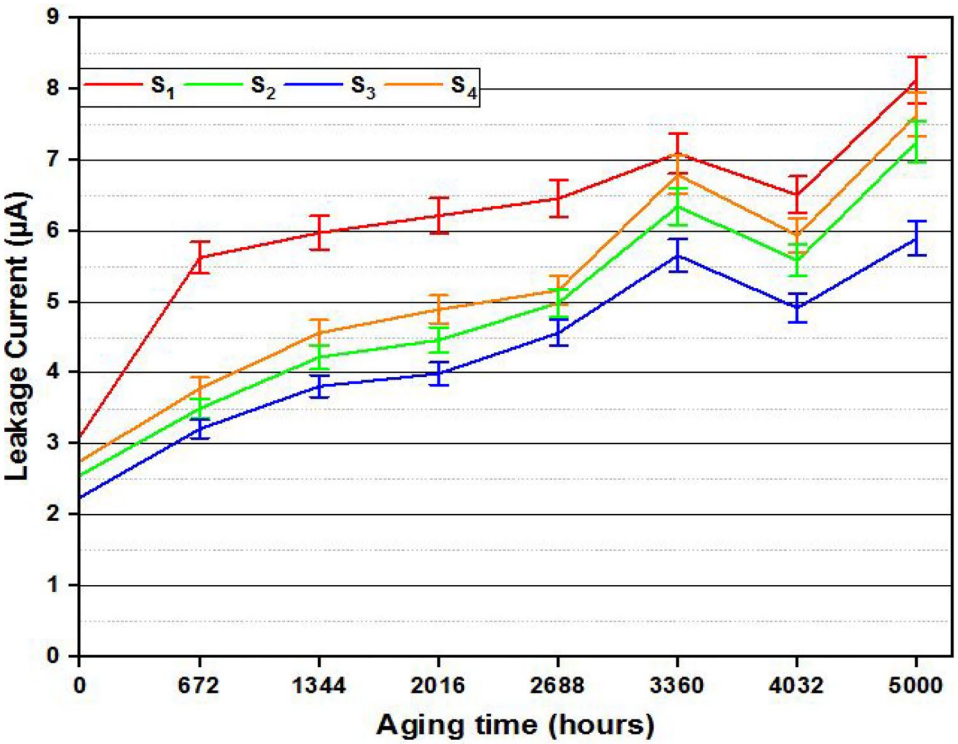


(b)

**Fig. 3** Leakage current measurements on HTV-SiR test samples aged under (**a**) negative DC and (**b**) positive DC voltages

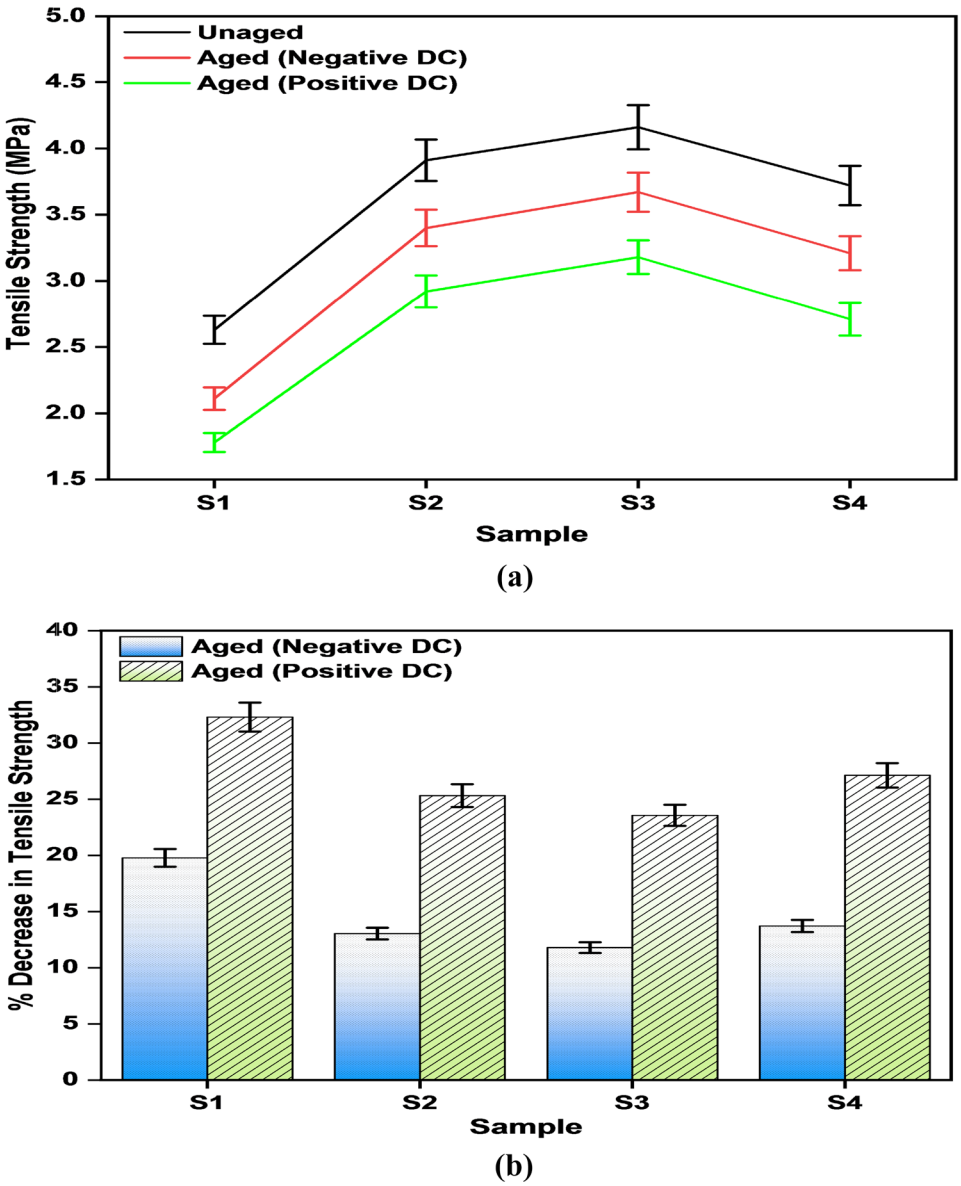


**Fig. 4** Sub-figure (**a**) shows tensile strength of the unaged test samples and aged materials under bipolar DC voltage while, sub-figure (**b**) represents %age decrease in tensile strength of the aged HTV-SiR materials

To quantify thermal stability of the test samples, temperature $T_{10}$ at which the samples lose their 10% weight is given in Table 3. Moreover, the residual mass in %age, termed as percent yield, is also presented in the same table. As seen, the value of $T_{10}$ is different for the studied materials being dependent on their composition. It is the lowest for unfilled sample $S_1$ and the highest for HTV-SiR $S_3$, containing 6 wt.% nano-silica and 15 wt.% micro-silica. Moreover, the change in $T_{10}$ brought about by aging is also affected by the composition of materials and polarity of the applied voltage. For sample $S_1$, variation is the maximum, while it is the minimum for sample $S_3$. Polarity effect is also consistent with the results of above-described diagnostic measurements e.g., positive DC stress imposes more influence compared to the negative DC. As far as percent yield is concerned, behavior of the test samples is similar as noted for temperature $T_{10}$. For instance, residual mass is more for sample $S_3$ than the other materials both in its unaged and aged conditions. Also, weight loss is higher under positive DC voltage compared to the negative DC.

Analyzing DTG curves of the unaged materials (sub-figures in the left column), it can be observed that the slope representing weight loss per degree rise in temperature is the maximum (go beyond − 0.5) for unfilled sample $S_1$ and the minimum (close to − 0.3) for hybrid composite $S_3$. Interestingly, the latter also shows two peaks, which may be attributed to the removal of micro- and nano-fillers from the base matrix in two different ranges of temperature. Contrarily, $S_2$ having relatively less amount of micro-silica exhibits only one peak. Curves of the remaining two samples $S_1$ and $S_4$

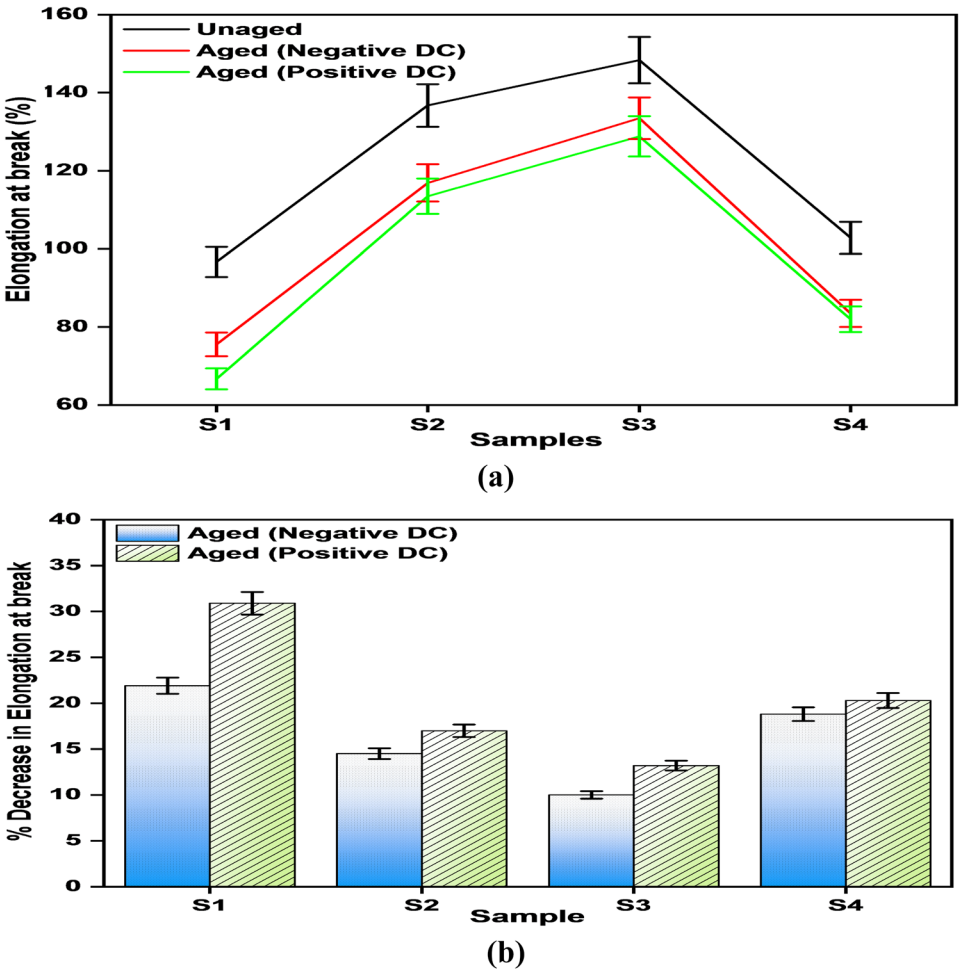


**Fig. 5** **a** Elongation at break (%) of the unaged test samples and aged materials under bipolar DC voltage and **b** % decrease in elongation at break of the aged HTV-SiR materials

also displays one peak. Apart from the composition, DTG curves are also affected by the aging conditions of the materials as well as by the polarity of DC voltage.

The above-described variation in TGA/DTG curves with the rise in temperature can be linked with the material decomposition, evaporation of volatile species, chain scission, etc. [55]. Consequently, a reduction in cross-linking as well as in the van der Waal's forces may occur particularly, at higher ambient temperature. Hence, from the TGA analysis, it is inferred that addition of hybrid filler (e.g., micro- and nano-silica) in certain proportion in the base material may affect its thermal characteristics considerably as validated by the results obtained for samples $S_3$ and $S_2$.

## Water immersion tests

Results of the 2-h boiling water immersion test at 100 ˚C and 24-h water immersion test at 25 ˚C are summarized in Tables 4 and 5, respectively. The corresponding increase in %age weight of the test samples is presented in Tables 6 and 7. Analyzing the data (Table 6) for virgin samples, it can be seen that the mass uptake is dependent on their composition. It is the highest (0.68%) for sample $S_1$ (without any additional filler) and the lowest (0.19%) for sample $S_3$, reinforced with hybrid filler containing 6 wt.% nano-silica and 15 wt.% micro-silica. The mass uptake also increases by exposing materials to environmental aging. Furthermore, this increment is higher under positive DC stress compared to the negative DC. For instance, for sample $S_1$, the percentage change under positive DC is 1.53, what that under negative DC is 1.25. Similar polarity effect can also be noticed for the other test samples as well.

Comparing percentage values in Table 6 with those in Table 7, it can be inferred that increase in mass uptake of the studied materials is more under 2-h boiling water immersion test than 24-h water immersion test. This tendency is the same regardless of the fact whether the samples are unaged or environmentally aged both under positive and negative DC stresses. The increase in sample's weight due to water absorption at high temperature may be linked with the enhancement in pre-existing voids [56]. Contrarily, high ambient temperature may also cause more loss of the LMW molecules due to their diffusing into liquid. Consequently, weight of the sample may reduce as is reported in [57].

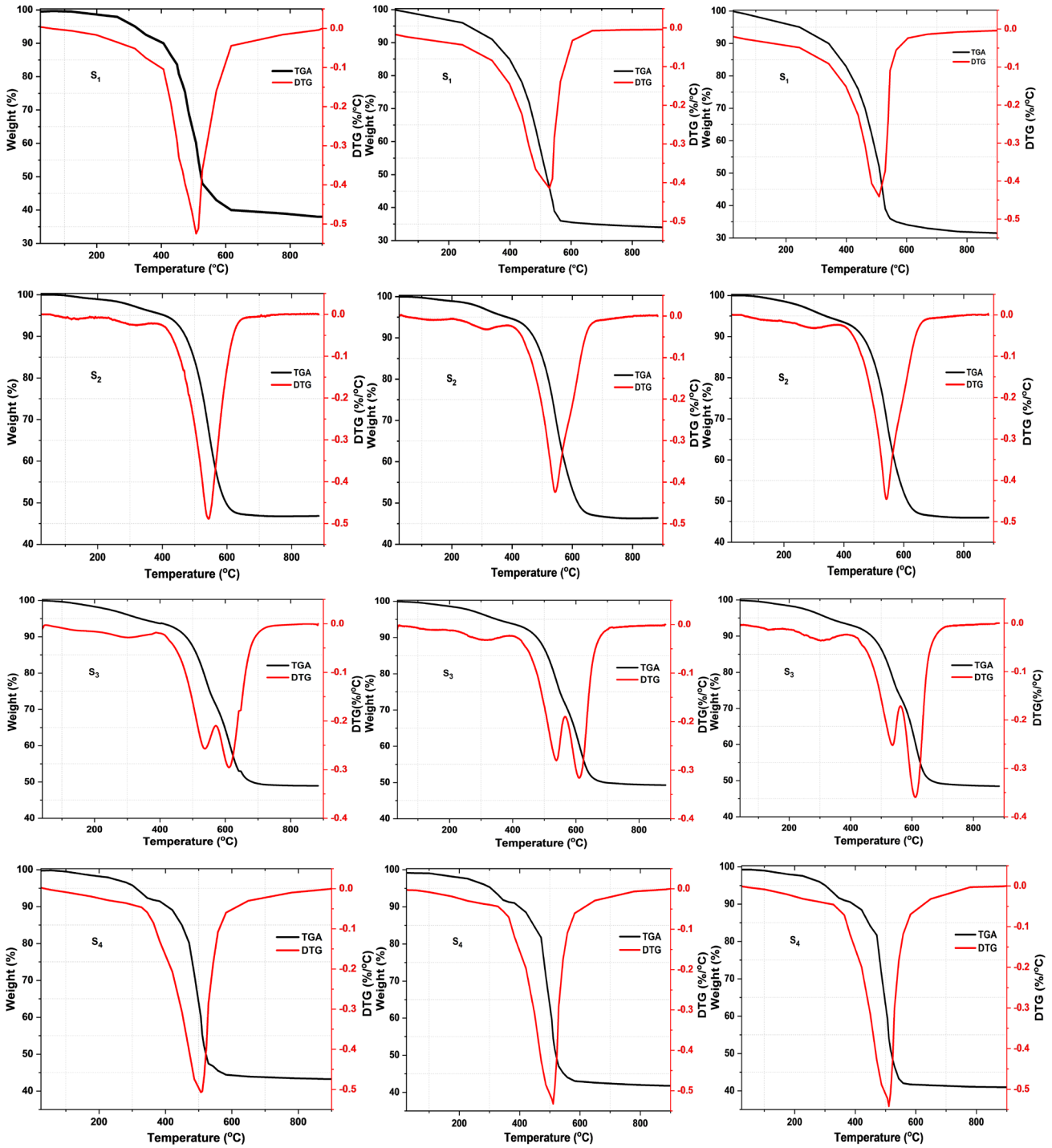


**Fig. 6** TGA/DTG curves of the studied test samples. Sub-figures in the left column show data for the unaged samples. While, those in the middle and right columns represent measurements for the materials aged under negative DC and positive DC voltages, respectively. Also, all the figures are labeled with the sample notation

Increase in the water permeation and mass uptake of the studied materials due to environmental aging can be associated with the loss of hydrophobic properties, resulting in their more attraction for water absorption [58]. It may also be attributed to the pre-existing voids in the samples, offering free space to be occupied by water molecules, degrading thus their electrical performance [59]. Among all the test samples, the co-filled materials $S_2$ and $S_3$ offered the highest resistance to water absorption due to stronger Van der Waal's forces and lower free volume on their surfaces.

**Table 3** Values of $T_{10}$ and percent yield of the test samples before and after their exposure to aging for 5000 h

| Sample | Temperature at 10% mass loss, ˚C | | | Percent yield | | |
|---|---|---|---|---|---|---|
| | Virgin (unaged) | Aged under negative DC | Aged under positive DC | Virgin (unaged) | Aged under negative DC | Aged under positive DC |
| $S_1$ | 408 | 355 | 342 | 41.6 | 38.6 | 35.7 |
| $S_2$ | 478 | 474 | 465 | 46.9 | 46.3 | 45.9 |
| $S_3$ | 485 | 482 | 476 | 49.3 | 48.9 | 48.4 |
| $S_4$ | 410 | 396 | 392 | 44.2 | 42.5 | 41.7 |

**Table 4** Results of the 2-h boiling water immersion test performed on the studied materials at 100 ˚C

| Test sample | Virgin (unaged) | | Aged under positive DC | | Aged under negative DC | |
|---|---|---|---|---|---|---|
| $S_1$ | 16.3 | 16.41 | 19.02 | 19.31 | 18.36 | 18.59 |
| $S_2$ | 18.07 | 18.12 | 18.86 | 18.93 | 18.75 | 18.81 |
| $S_3$ | 15.94 | 15.97 | 19.31 | 19.37 | 19.77 | 19.82 |
| $S_4$ | 17.7 | 17.78 | 18.66 | 18.77 | 18.45 | 18.53 |

Values in the left and right columns under each category represent mass (in gram) of the samples before and after the test, respectively

**Table 5** Results of the 24-h water immersion test performed on the studied materials at 25 ˚C

| Test sample | Virgin (unaged) | | Aged under positive DC | | Aged under negative DC | |
|---|---|---|---|---|---|---|
| $S_1$ | 16.21 | 16.31 | 16.82 | 17.05 | 17.65 | 17.85 |
| $S_2$ | 18.12 | 18.16 | 18.93 | 18.99 | 18.86 | 18.91 |
| $S_3$ | 15.99 | 16.01 | 19.38 | 19.42 | 19.84 | 19.87 |
| $S_4$ | 17.65 | 17.72 | 18.33 | 18.42 | 18.99 | 19.08 |

Values in the left and right columns under each category represent mass (in gram) of the samples before and after the test, respectively

**Table 6** Percentage increase in mass uptake during 2-h boiling water immersion test on the unaged samples and aged materials under bipolar DC voltage for 5000 h

| Test sample | Virgin (unaged) | Aged under positive DC | Aged under negative DC |
|---|---|---|---|
| $S_1$ | 0.68 | 1.53 | 1.25 |
| $S_2$ | 0.28 | 0.37 | 0.32 |
| $S_3$ | 0.19 | 0.31 | 0.25 |
| $S_4$ | 0.45 | 0.59 | 0.54 |

**Table 7** Percentage increase in mass uptake during 24-h water immersion test on the unaged samples and aged materials under bipolar DC voltage for 5000 h

| Sample | Virgin (unaged) | Aged under positive DC | Aged under negative DC |
|---|---|---|---|
| $S_1$ | 0.61 | 1.37 | 1.13 |
| $S_2$ | 0.22 | 0.32 | 0.26 |
| $S_3$ | 0.13 | 0.21 | 0.15 |
| $S_4$ | 0.39 | 0.49 | 0.47 |

## FTIR spectroscopic analysis

FTIR spectra, displaying absorbance vs. wavenumbers, of the studied materials before and after their aging under multiple stresses is shown in Fig. 7. As seen, there exist four peaks corresponding to important functional groups, associated with the desired properties (electrical, mechanical, etc.) of polymeric materials [60], within different wavenumber ranges. Information about these is summarized in Table 8. Inferring the curves (in sub-figures) for virgin samples, it can be seen that maximum values of the absorption peaks are different, being dependent on their compositions. For instance, hybrid filled silicone rubber $S_3$ attains the highest values, while unfilled sample $S_1$ the lowest. For other two materials, these are in-between.

By comparing the curves of aged samples with those of the unaged, a decrease in the absorption peaks of all the chemical groups can be noticed. The reason being their degradation due to the impact of environmental and electrical stresses as reported in [61]. To quantify the %age decrease, values calculated with respect to the data obtained for virgin

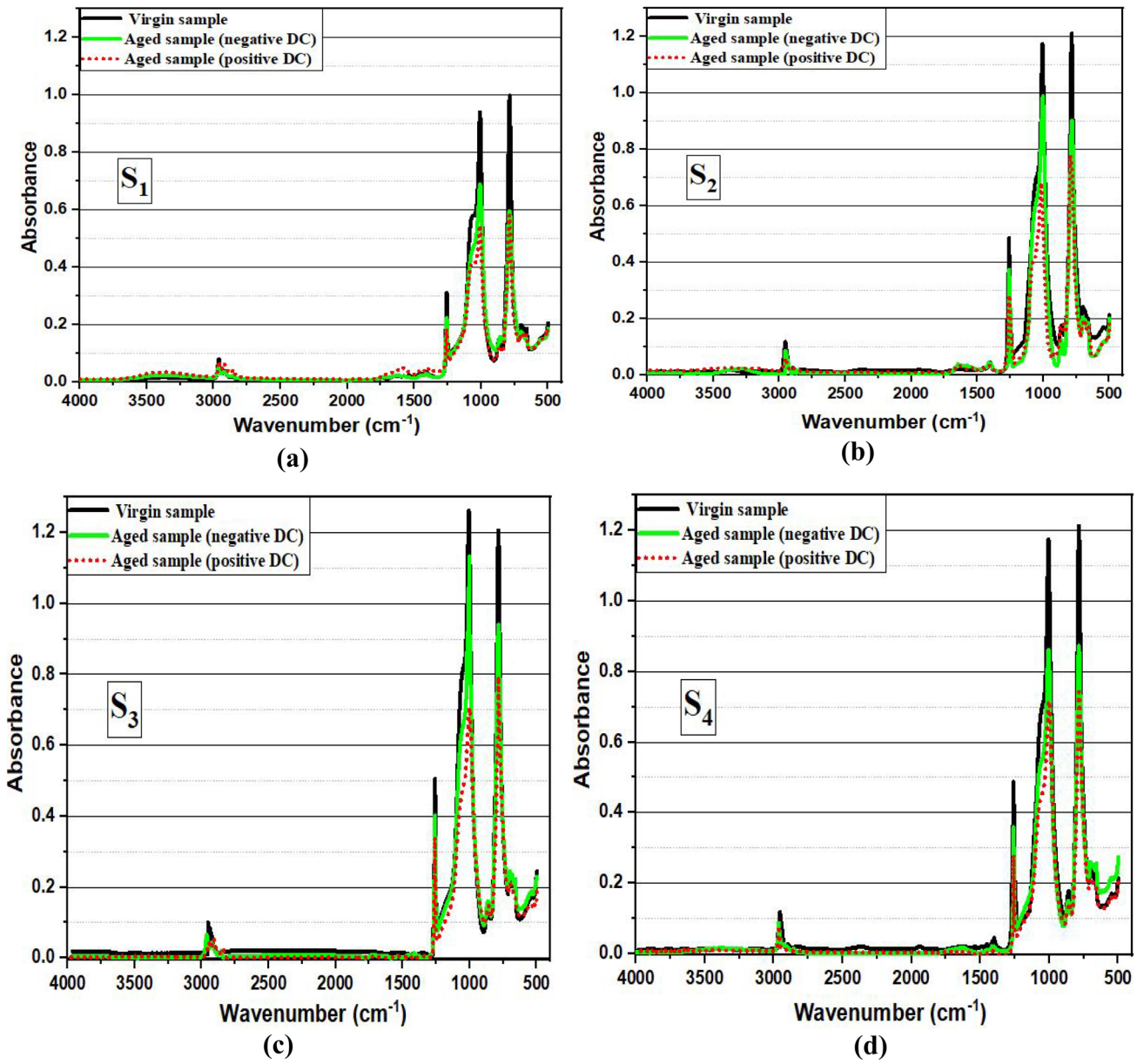


**Fig. 7** FTIR spectra of the virgin (unaged) samples and aged materials under multiple environmental stresses and bipolar DC voltage for 5000 h. Sub-figures are labeled with the sample notation

samples are presented in the last two columns of Table 8. As seen, the numbers (representing %age loss in absorption peak) are the highest for sample $S_1$ (without any filler) and the lowest for sample $S_3$ (filled with 6 wt.% nano-silica and 15 wt.% micro-silica) for all the functional groups. The loss in absorption peaks of other two materials $S_2$ and $S_4$ is in between those for samples $S_1$ and $S_3$. Moreover, among the four chemical groups, the highest decrease in absorption peaks is obtained for Si–$CH_3$ and the lowest for Si–O–Si. As far as severity of the impact associated with the polarity of the applied voltage is concerned, it is more under positive DC stress than the negative DC. The above-described results indicated relatively better performance of the hybrid composites compared to the other studied formulations, which may be attributed to the fine silica particles dispersion, resulting in their strong interaction with the polymer base matrix [62].

## SEM analysis

SEM micrographs of the test samples were taken at a magnification level of 1000 following the procedure outlined

**Table 8** Percentage decrease in absorption peaks of the functional groups of aged silicone rubbers for 5000 h calculated with respect to the data obtained for virgin samples

| Samples | Functional groups | Wavenumber ($cm^{-1}$) | Decrease in absorption peaks of aged samples, % | |
|---|---|---|---|---|
| | | | Aged under positive DC voltage | Aged under negative DC voltage |
| $S_1$ | Si $(CH_3)_2$ | 790–840 | 43 | 40 |
| $S_2$ | | | 36.1 | 26.2 |
| $S_3$ | | | 33.9 | 21.5 |
| $S_4$ | | | 38.1 | 27.3 |
| $S_1$ | Si–O–Si | 1000–1130 | 42.1 | 28.4 |
| $S_2$ | | | 41.5 | 15.3 |
| $S_3$ | | | 37 | 11.1 |
| $S_4$ | | | 42 | 26.9 |
| $S_1$ | Si–$CH_3$ | 1255–1280 | 45.4 | 27.3 |
| $S_2$ | | | 40.8 | 22.5 |
| $S_3$ | | | 31.4 | 21.6 |
| $S_4$ | | | 42.8 | 24.5 |
| $S_1$ | C–H in $CH_3$ | 2960–2963 | 36.4 | 32.3 |
| $S_2$ | | | 33.3 | 28.9 |
| $S_3$ | | | 30 | 26.3 |
| $S_4$ | | | 35.2 | 29.7 |

in Sect. "SEM Analysis". The collected data for virgin (unaged) materials are shown in Fig. 8. While, images of the environmentally aged samples under negative and positive DC voltages are displayed in Fig. 9 and Fig. 10, respectively. Analyzing micrographs of the unaged samples, fairly smooth surfaces can be observed. Even though, depending on the composition, there also exist signs of only moderate level of surface roughness due to addition of filler particles in the base matrix. On the other hand, samples exposed to different types of stresses in the environmental chamber for a duration of 5000 h exhibit noticeable surface degradation in the form of cracks and block like structures. These results in high surface roughness, the severity of which is affected by both the sample's composition and polarity of the applied voltage. For instance, sample $S_1$ (without any filler) under negative DC voltage displays cracks of shallow type over the entire surface. While, under positive DC voltage, it shows deep cracks and surface splits into discrete blocks. Other studied materials also show similar characteristics. Such irregularities can mainly be associated with the chain scission of base matrix and surface oxidation brought about by UV radiations, electrical stresses, high temperature and humidity [63, 64]. Among the investigated formulations, hybrid composite $S_3$ (containing 6 wt.% nano-silica and 15 wt.% micro-silica) offered the highest resistance against surface

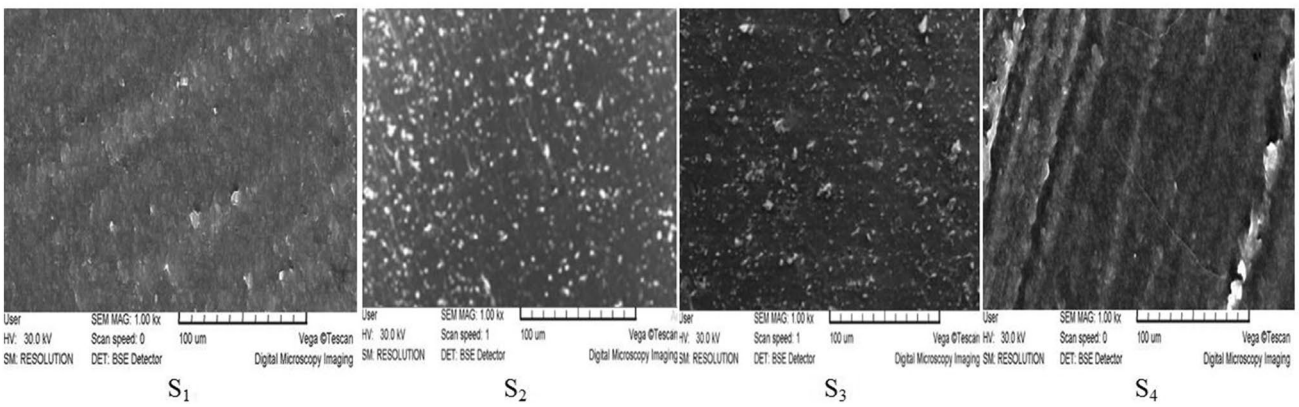


**Fig. 8** SEM images of the unaged samples of HTV silicone rubber. Sub-figures are labeled with the sample notation

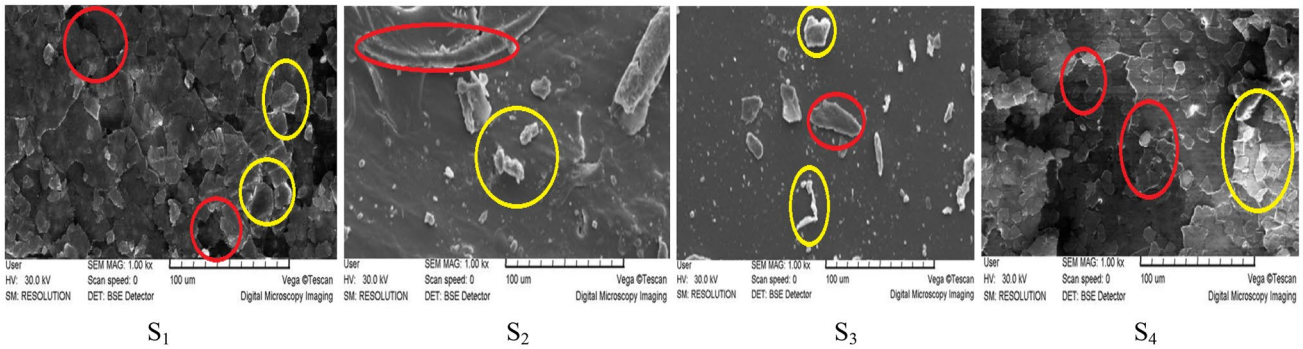


**Fig. 9** SEM images of the environmentally aged samples under negative DC voltage. Signs of degradation (e.g., cracks, block like structures) are indicated with the red and yellow circles

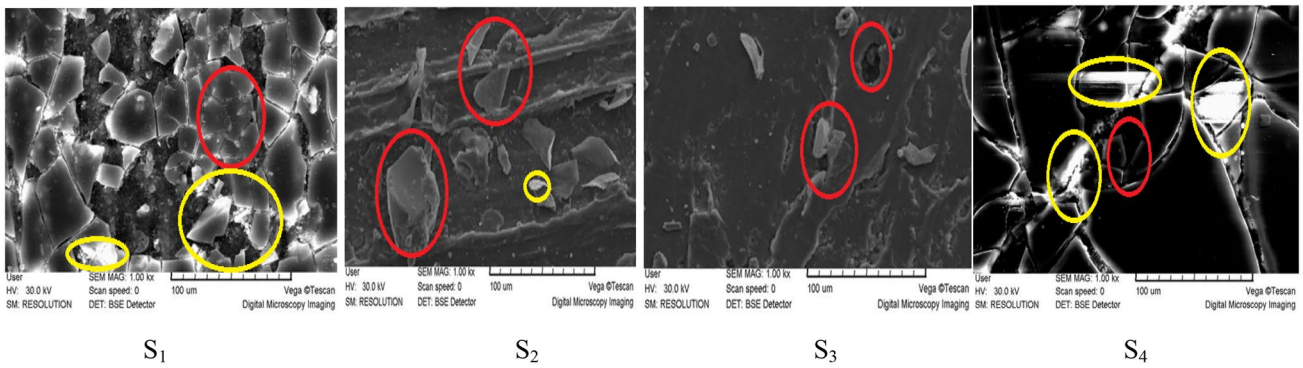


**Fig. 10** SEM images of the environmentally aged samples under positive DC voltage. Signs of degradation (e.g., cracks, block like structures) are indicated with the red and yellow circles

degradation/roughness due to aging, showing thus good potential for high voltage outdoor applications.

## Conclusion

The present research work was conducted to assess performance of several types of composites, made of HTV-SiR and micro- and nano-sized silica filler. Following by preparation of the test samples, they were exposed to different environmental stresses/factors (temperature, humidity, UV radiation, acid rain and salt-fog) and bipolar DC voltage for a duration of 5000 h. Thereafter, the aged materials were diagnosed through different techniques to check their integrity in terms of electrical, mechanical, thermal, chemical and morphological properties as well as surface characteristics. Results of the performed measurements and allied analysis exhibited that severity of degradation is suppressed better by hybrid filled composites compared to the other investigated formulations. Moreover, impact created by the positive DC stress was found higher than the negative DC. Among the studied materials, HTV-SiR reinforced with 6 wt.% nano-silica and 15 wt.% micro-silica offered the strongest opposition to aging. Hence, this composition shows good potential for high voltage outdoor insulation in DC transmission lines with better performance and extended life.

## Declarations

**Conflict of interest** The authors declare no conflict of interest.

## References

1. Bahrman MP (2006) Overview of HVDC transmission. IEEE PES Power Syst Conf Exposition 2006:18–23
2. Zhou X, Chen S, Lu Z (2013) Review and prospect for power system development and related technologies: a concept of three-generation power systems. Proc CSEE 33:1–11
3. Long W, Nilsson S (2007) HVDC transmission: yesterday and today. IEEE Power Energ Mag 5:22–31
4. Kannan P, Sivakumar M, Mekala K, Chandrasekar S (2015) Tracking/erosion resistance analysis of Nano-Al$(OH)_3$ filled silicone rubber insulating materials for high voltage dc applications. J Electr Eng Technol 10:355–363

5. Moreno V, Gorur R (1999) AC and DC performance of polymeric housing materials for HV outdoor insulators. IEEE Trans Dielectr Electr Insul 6:342–350
6. Bruce G, Rowland S, Krivda A (2010) Performance of silicone rubber in DC inclined plane tracking tests. IEEE Trans Dielectr Electr Insul 17:521–532
7. Ehsani M, Borsi H, Gockenbach E, Morshedian J, Bakhshandeh G (2004) An investigation of dynamic mechanical, thermal, and electrical properties of housing materials for outdoor polymeric insulators. Eur Polymer J 40:2495–2503
8. Hergert A, Kindersberger J, Bär C, Bärsch R (2017) Transfer of hydrophobicity of polymeric insulating materials for high voltage outdoor application. IEEE Trans Dielectr Electr Insul 24:1057–1067
9. Reynders J, Jandrell I, Reynders S (1999) Review of aging and recovery of silicone rubber insulation for outdoor use. IEEE Trans Dielectr Electr Insul 6:620–631
10. Chen WJ, Zeng X, Lai X, Li H, Fang WZ, Hou F (2016) Suppression effect and mechanism of platinum and nitrogen-containing silane on the tracking and erosion of silicone rubber for high-voltage insulation. ACS Appl Mater Interfaces 8:21039–21045
11. Nazir MT, Khalid A, Wang C, Baena JC, Kabir I, Akram S et al (2022) Synergistic effect of additives on electrical resistivity, fire and smoke suppression of silicone rubber for high voltage insulation. Composites Commun 29:101045
12. Deng H, Hackam R (1999) Low-molecular weight silicone fluid in RTV silicone rubber coatings. IEEE Trans Dielectr Electr Insul 6:84–94
13. Kim S-H, Cherney E, Hackam R (1991) Suppression mechanism of leakage current on RTV coated porcelain and silicone rubber insulators. IEEE Trans Power Delivery 6:1549–1556
14. Siderakis K, Agoris D (2008) Performance of RTV silicone rubber coatings installed in coastal systems. Electr Power Syst Res 78:248–254
15. Mehmood B, Akbar M, Ullah R (2021) Water absorption resistance study of HTV silicone rubber-based hybrid composites. Int Conf Emerging Power Technol (ICEPT) 2021:1–5
16. Gubanski S Erosion resistance of different housing materials to UV irradiation and surface discharges action, In: 1988 Fifth International Conference on Dielectric Materials, Measurements and Applications, 1988, pp. 37–40.
17. Jawaid M, Thariq M, Saba N Durability and life prediction in biocomposites, fibre-reinforced composites and hybrid composites, Woodhead Publishing, 2018.
18. Momen G, Farzaneh M (2011) Survey of micro/nano filler use to improve silicone rubber for outdoor insulators. Rev Adv Mater Sci 27:1–13
19. Nazir MT, Butt FT, Hussain H, Phung BT, Akram S, Bhutta MS et al (2022) Physical, thermal and partial discharge evaluation of nano alumina filled silicone rubber in an inclined plane test. CSEE J Power Energy Syst 8:1242
20. Ansorge S, Schmuck F, Papailiou KO (2015) Impact of different fillers and filler treatments on the erosion suppression mechanism of silicone rubber for use as outdoor insulation material. IEEE Trans Dielectr Electr Insul 22:979–988
21. Venkatesulu B, Thomas MJ (2010) Erosion resistance of alumina-filled silicone rubber nanocomposites. IEEE Trans Dielectr Electr Insul 17:615–624
22. Anhalt M, Weidenfeller B (2011) Influence of filler content, particle size and temperature on thermal diffusivity of polypropylene-iron silicon composites. J Appl Polym Sci 119:732–735
23. El-Hag A, Jayaram S, Cherney E (2004) Comparison between silicone rubber containing micro-and nano-size silica fillers [insulating material applications]," in *The 17th Annual Meeting of the IEEE Lasers and Electro-Optics Society, 2004*. LEOS 2004:385–388
24. Nazir MT, Phung BT, Yeoh GH, Yasin G, Akram S, Bhutta MS et al (2020) Enhanced dielectric and thermal performance by fabricating coalesced network of alumina trihydrate/boron nitride in silicone rubber for electrical insulation. Bull Mater Sci 43:1–5
25. Akram S, Gao G, Liu Y, Zhu J, Wu G, Zhou K (2015) Degradation mechanism of $Al_2O_3$ nano filled polyimide film due to surface discharge under square impulse voltage. IEEE Trans Dielectr Electr Insul 22:3341–3349
26. Khattak A, Amin M (2016) Influence of stresses and fillers on the aging behaviour of polymeric insulators. Rev Adv Mater Sci 44:194–205
27. Aman A, Yaacob MM, Alsaedi MA, Ibrahim KA (2013) Polymeric composite based on waste material for high voltage outdoor application. Int J Electr Power Energy Syst 45:346–352
28. El-Hag A, Simon L, Jayaram S, Cherney E (2006) Erosion resistance of nano-filled silicone rubber. IEEE Trans Dielectr Electr Insul 13:122–128
29. Nazir MT, Phung B, Li S (2017) Erosion resistance of micro-AlN and nano-$SiO_2$ hybrid filled silicone rubber composites. Int Symp Electr Insulating Materials (ISEIM) 2017:370–373
30. Akbar M, Ullah R, Karim MA (2020) Interpreting surface degradation of HTV silicone rubber filled with micro/nano-silica under AC and DC voltages. J Electron Mater 49:5399–5410
31. Amin M, Khattak A, Ali M (2018) Accelerated aging investigation of silicone rubber/silica composites for coating of high-voltage insulators. Electr Eng 100:217–230
32. Sundararajan R, Graves J, Mohammed A, Baker A, Performance evaluation of polymeric insulators aged in lab and field. In: 2003 IEEE Power Engineering Society General Meeting (IEEE Cat. No. 03CH37491), 2003, pp. 219–224.
33. Yoshimura N, Kumagai S, Nishimura S (1999) Electrical and environmental aging of silicone rubber used in outdoor insulation. IEEE Trans Dielectr Electr Insul 6:632–650
34. Rashid A, Amin M, Ali M, Khattak A (2018) Aging exploration of long term multistressed HTV-silicone rubber/silica/alumina composites for high voltage insulation. Materials Res Express 5:095301
35. Du B, Li Z, Yang Z (2016) Field-dependent conductivity and space charge behavior of silicone rubber/SiC composites. IEEE Trans Dielectr Electr Insul 23:3108–3116
36. Cheng L, Wang L, Guan Z, Zhang F (2016) Aging characterization and lifespan prediction of silicone rubber material utilized for composite insulators in areas of atypical warmth and humidity. IEEE Trans Dielectr Electr Insul 23:3547–3555
37. Butt FT, Nazir MT, Hussain H, Phung BT, Akram S, Bhutta MS et al. Physical, thermal and partial discharge evaluation of nano alumina filled silicone rubber in inclined plane test. In: CSEE J Power Energy Syst 2020.
38. Nazir MT, Phung B, Li S, Akram S, Mehmood MA, Yeoh G et al (2019) Effect of micro-nano additives on breakdown, surface tracking and mechanical performance of ethylene propylene diene monomer for high voltage insulation. J Mater Sci 30:14061–14071
39. Nazir MT, Nazir MS, Jiang XL, Akram S (2012) Performance of De-Energized Polymeric Insulating Material under Various Environment Stresses. In: Advanced Materials Research, pp. 60–63.
40. Li Q-f, Su Z-y (2006) 5000 h artificial accelerating ageing test of HVDC composite insulator. Power Syst Technol 12
41. Liang X, Zhang Y, Yin Y, Li Z (2012) 5000 h multi-stress test procedure for silicone rubber composite insulators and its applications in long- term performance evaluation. Gaodianya Jishu/High Voltage Eng 38:2492–2498
42. Akbar M, Ullah R, Qazi I (2020) Multi-stress aging investigations of HTV silicone rubber filled with Silica/ATH composites for HVAC and HVDC transmission. Eng Fail Anal 110:104449

43. Standard I (1992) Composite insulators for AC overhead lines with nominal voltage greater than 1000 V-definitions, test methods and acceptance criteria. IEC 1109:03
44. Guide S (1992) 92/1 Hydrophobicity classification guide, Swedish Trans Res Inst.
45. Nandi S, Reddy BS, Sharma D (2019) Performance of composite insulators used for electric transmission under extreme climatic conditions. J Mater Eng Perform 28:5959–5969
46. Standard A (2018) Standard test method for water absorption of plastics. ASTM D570–95, ed.
47. A. S. f. (2010) Testing and Materials–ASTM, ASTM D570-98–Standard Test Method for Water Absorption of Plastics.
48. Kim J, Chaudhury M, Owen M (1999) Hydrophobicity loss and recovery of silicone HV insulation. IEEE Trans Dielectr Electr Insul 6:695–702
49. Hillborg H, Gedde U (1999) Hydrophobicity changes in silicone rubbers. IEEE Trans Dielectr Electr Insul 6:703–717
50. Koné D, Ghunem RA, Cissé L, Hadjadj Y, El-Hag AH (2019) Effect of residue formed during the AC and DC dry-band arcing on silicone rubber filled with natural silica. IEEE Trans Dielectr Electr Insul 26:1620–1626
51. Heger G, Vermeulen H, Holtzhausen J, Vosloo W (2010) A comparative study of insulator materials exposed to high voltage AC and DC surface discharges. IEEE Trans Dielectr Electr Insul 17:513–520
52. Zong Y, Gui D, Li S, Tan G, Xiong W, Liu J Preparation and thermo-mechanical properties of functionalized graphene/silicone rubber nanocomposites. In: 2015 16th International Conference on Electronic Packaging Technology (ICEPT), 2015, pp. 30–34.
53. Nazir MT, Phung B, Hoffman M (2016) Performance of silicone rubber composites with $SiO_2$ micro/nano-filler under AC corona discharge. IEEE Trans Dielectr Electr Insul 23:2804–2815
54. Wietzke S, Jansen C, Reuter M, Jung T, Kraft D, Chatterjee S et al (2011) Terahertz spectroscopy on polymers: A review of morphological studies. J Mol Struct 1006:41–51
55. Zhou WY, Qi SH, Zhao HZ, Liu NL (2007) Thermally conductive silicone rubber reinforced with boron nitride particle. Polym Compos 28:23–28
56. Wang J, Gong J, Gong Z, Yan X, Wang B, Wu Q et al (2010) Effect of curing agent polarity on water absorption and free volume in epoxy resin studied by PALS. Nucl Instrum Methods Phys Res, Sect B 268:2355–2361
57. Khattak A Long term multistress aging of high voltage nanocomposites, COMSATS Institute of Information Technology Islamabad-Pakistan, 2017.
58. Wang Z, Jia Z, Fang M, Guan Z (2015) Absorption and permeation of water and aqueous solutions of high-temperature vulcanized silicone rubber. IEEE Trans Dielectr Electr Insul 22:3357–3365
59. Ullah I, Amin M, Nazir MT, Hussain H (2020) Impact of accelerated ultraviolet weathering on polymeric composite insulators under high voltage DC stress. CSEE Journal of Power and Energy Systems.
60. Verma AR, Reddy BS (2018) Tracking and erosion resistance of LSR and HTV silicon rubber samples under acid rain conditions. IEEE Trans Dielectr Electr Insul 25:46–52
61. Mehmood B, Akbar M, Ullah R (2020) Accelerated aging effect on high temperature vulcanized silicone rubber composites under DC voltage with controlled environmental conditions. Eng Fail Anal 118:104870
62. Lau KY, Piah M (2011) Polymer nanocomposites in high voltage electrical insulation perspective: a review. Malaysian Polymer Journal 6:58–69
63. Ullah I, Akbar M, Khan HA (2022) Enhancement of electrical, mechanical and thermal properties of silicone based coating with aluminatrihydrate/silica for ceramic insulators. Mater Chem Phys 282:125972
64. Wen X, Yuan X, Lan L, Hao L, Wang Y, Li S et al (2017) RTV silicone rubber degradation induced by temperature cycling. Energies 10:1054